Proceedings of ASME Turbo Expo 2016: Turbomachinery Technical Conference and Exposition
GT2016
June 13 – 17, 2016, Seoul, South Korea

GT2016-56168

THE ROLE OF IMPELLER OUTFLOW CONDITIONS ON THE PERFORMANCE OF VANED DIFFUSERS

Jonathan Everitt*,
Zoltán Spakovszky
Massachusetts Institute of Technology,
Cambridge, MA, USA

Daniel Rusch
ABB Turbo Systems Ltd,
Baden, Switzerland

Jürg Schiffmann
École Polytechnique Fédérale de Lausanne,
Lausanne, Switzerland

ABSTRACT

Highly-loaded impellers, typically used in turbocharger and gas turbine applications, exhaust an unsteady, transonic flow that is non-uniform across the span and pitch and swirling at angles approaching tangential. With the exception of the flow angle, conflicting data exist regarding whether these attributes have substantial influence on the performance of the downstream diffuser.

This paper quantifies the relative importance of the flow angle, Mach number, non-uniformity and unsteadiness on diffuser performance, through diffuser experiments in a compressor stage and in a rotating swirling flow test rig. This is combined with steady and unsteady Reynolds-Averaged Navier Stokes computations. The test article is a pressure ratio 5 turbocharger compressor with an airfoil vaned diffuser. The swirling flow rig is able to generate rotor outflow conditions representative of the compressor except for the periodic pitchwise unsteadiness, and fits a 0.86 scale diffuser and volute. In both rigs, the time-mean impeller outflow is mapped across a diffuser pitch using miniaturized traversing probes developed for the purpose.

Across approximately two-thirds of the stage operating range, diffuser performance is well correlated to the average impeller outflow angle when the metric used is effectiveness, which describes the pressure recovery obtained relative to the maximum possible given the average inflow angle, Mach number and the vane exit metal angle. Utilizing effectiveness captures density changes through the diffuser at higher Mach numbers; a 10% increase in pressure recovery is observed as the inlet Mach number is increased from 0.5 to 1. Further, effectiveness is shown to be largely independent of the time-averaged spanwise and unsteady pitchwise non-uniformity from the rotor; this independence is reflective of the strong mixing processes that occur in the diffuser inlet region. The observed exception is for operating points with high time-averaged vane incidence. Here, it is hypothesized that temporary excursions into high-loss flow regimes cause a non-linear increase in loss as large unsteady angle variations pass by from the rotor.

Given that straight-channel diffuser design charts typically used in preliminary radial vaned diffuser design capture neither streamtube area changes from impeller exit to the diffuser throat nor vane incidence effects, their utility is limited. An alternative approach, utilizing effectiveness and vane leading edge incidence, is proposed.

INTRODUCTION

Modern high pressure ratio centrifugal compressors typically utilize a high speed impeller with backswept blades and a vaned diffuser. As part of ongoing efforts for a system-wide reduction in weight, increase in efficiency and/or reduction of emissions, designers seek to improve the pressure ratio, operating range and efficiency of the centrifugal compressor, which is often limited by the diffuser. Despite the relative simplicity of its geometry, the flow in the diffuser is complex and there is no well-established, reliable approach to guide design for these goals.

For the purposes of preliminary design of vaned diffusers, the flow is frequently approximated as two-dimensional: either that of straight-channel, quasi-1D diffusers (allowing use of diffuser design charts such as those by Reneau [1]) or geometrically transformed cascade airfoils (e.g. [2]). This is despite their apparent limitations; various techniques must be employed to correct for the clear differences in geometry as well as for the effects of incidence on to the diffuser vanes. Additionally, the empirical data shows insensitivity to Mach number, in conflict with the expected results from quasi-1D flow theory, and a strong dependence on throat blockage, which is difficult to quantify (or avoid) in centrifugal compressor

* Current address: Altaeros Energies Inc., 28 Dane St., Somerville, MA, 02143

diffusers. As a consequence, the usefulness of these approaches is questionable; for example, using cascade airfoil data severely underestimates loss [2].

In a two-part paper, Filipenco and Deniz et al. [3,4] argue that radial vaned diffuser pressure recovery performance correlate uniquely to the momentum averaged inflow angle, as long as the pressure recovery coefficient is defined using the "availability average" inflow total pressure. This method of averaging best captures the relevant flow quantities for the diffuser, and under most flow conditions is very similar to the mass flow average [5]. Given this correlation has no direct dependence on blockage, they suggest that designing for low blockage at diffuser inlet has no advantage, providing that the diffuser is designed to operate at an appropriate mean inflow angle. The conclusion is based on data taken for high solidity diffusers in a swirling flow test rig, using inflow parameters determined to be representative of high pressure ratio gas turbine engine centrifugal compressors. Their generality to real compressors, or to different diffuser geometries, is unclear.

When applied to the diffuser studied in this paper, the correlation of pressure recovery to the momentum-averaged flow angle is significantly worse than observed by Filipenco or Deniz, as indicated in Figure 1 (scales are removed to protect proprietary data). Here the pressure recovery coefficient across the diffuser, defined as:

$$C_p = \frac{p_5 - p_{2a}}{\bar{p}^m_{t,2a} - p_{2a}} \qquad (1)$$

is plotted against the momentum averaged inflow angle, such that left-to-right represents a compressor speedline throttled in to stall. The spread in C_p at the penultimate operating point before stall is 18%. The derivation of this experimental data is described later in the paper.

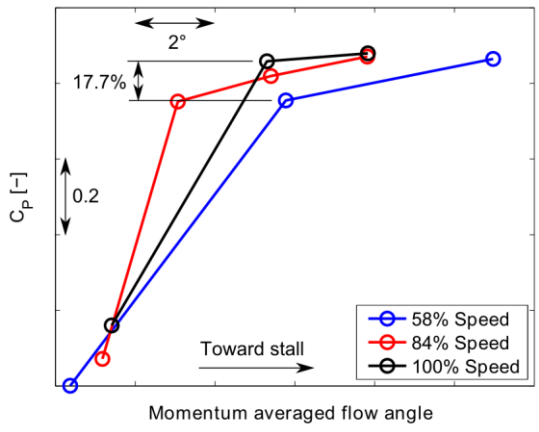

Figure 1: Experimentally determined pressure recovery coefficient C_p for the research diffuser, as a function of momentum averaged angle as defined by Filipenco et al. [3] showing relatively poor correlation.

In contrast to Filipenco and Deniz, who determined that the non-uniformity in the spanwise direction had little impact on the diffuser pressure recovery performance, Spakovszky and Roduner [6] demonstrate that both pressure recovery and stable flow range can be highly sensitive to flow leakage at impeller exit. The pre-production compressor investigated in that paper is of aggressive design, pushing the limits in stage matching. The leakage flow, used for thrust balance and bearing compartment sealing, is suggested to have a profound effect on component matching with changes in one-dimensional corrected flow overriding any potential effects of spanwise flow non-uniformity.

The unsteady impeller outflow has been characterized using URANS simulations or PIV/LDV by several researchers e.g. [7-10]. It is generally agreed that the effects of this unsteady flow on diffuser performance are limited at design conditions. However, little data exists at off-design conditions. Baghdadi [11] compared diffuser performance within a stationary swirling flow rig to a compressor rig and determined differences were small, but inflow measurements were limited. Clear design guidelines arising from these studies are lacking, and it is evident that unsteady CFD remains too computationally expensive, both in solution time and post-processing, to be part of the routine design cycle.

SCOPE OF PAPER

The goal of this paper is to quantify the relative significance of different flow features present in the inflow of radial vaned diffusers, in terms of their influence on steady-state diffuser performance (pressure recovery and loss). These flow features are the average inflow angle and Mach number, the time-averaged spanwise flow non-uniformity (or blockage), and the unsteady pitchwise flow non-uniformity. At the outset of the project, the following hypotheses were postulated: (a) the unsteadiness of the diffuser inflow, caused by the pitchwise non-uniformity imposed by the rotating impeller upstream, has negligible influence on the diffuser aerodynamics, consistent with the prevailing consensus in the literature [12]; (b) the spanwise flow non-uniformity, considered in a time-averaged sense, impacts the flow aerodynamics in the diffuser inlet region (inlet to diffuser throat) and hence the overall diffuser performance and stall characteristics; and (c) that the effects of Mach number should be measurable in the performance of the diffuser.

The approach taken combines a series of experiments in two experimental facilities. Unique to this research, comprehensive data has been taken on a swirling flow test rig together with a compressor test bed, using the same radial vaned diffuser as a test article. This allows the influence of the diffuser inflow features to be isolated in the steady state diffuser performance. In addition, this data are supported by computational simulations using steady and unsteady RANS, allowing additional interrogation of the flow features.

This work indicates incidence onto the diffuser vanes is a primary driver of diffuser performance, with greater sensitivity as Mach numbers increase. The time-average spanwise non-uniformity into the diffuser has little impact on the diffuser performance except as it affects the mixed out average conditions. Additionally, unsteadiness arising from the

upstream impeller has the greatest effect on the diffuser at off-design conditions, where it is proposed that large temporal flow angle variations give rise to worse performance due to the highly non-linear relationship between loss and incidence. For a large proportion of the operating range, it is shown to have little impact. The work develops, and then uses, a compressible definition of diffuser effectiveness as a performance metric, using a mixed-out condition as a means of characterizing the diffuser inflow.[1]

NOMENCLATURE

A	Area
A_{eff}	Effective area
b	Passage height / span
bpf	Blade passing frequency
c_p	Specific heat at constant pressure
C_p	Static pressure recovery coefficient
$C_{p,t}$	Total pressure loss coefficient
CFD	Computational Fluid Dynamics
CH	Near choke operating point
$D(M)$	Compressible flow function $\frac{\dot{m}\sqrt{c_p T_t}}{A p_t}$
$\dot{m}$	Mass flow
M	Mach number
p	Static pressure
p_t	Total pressure
$\bar{p}_t^m$	Mass averaged total pressure
r	Radius
Re	Diffuser Reynolds number $\frac{\rho_{2a} u_{2a} b_{2a}}{\mu_{2a}}$
ST	Near stall operating point
T_t	Total temperature
u	Flow velocity
[U]RANS	[Unsteady] Reynolds Averaged Navier Stokes
z	Axial coordinate (spanwise at diffuser inlet)
α	Flow angle, from radial
γ	Ratio of specific heats
η_{max}	Near maximum efficiency operating point
θ	Circumferential coordinate (pitchwise at diffuser inlet)
ρ	Density
χ	Blade metal angle, from radial
Ω	Impeller rotational speed

Compressor stations

1	Impeller leading edge axial plane
2	Impeller trailing edge radius
2a	Diffuser inlet measurement plane
3	Diffuser leading edge radius
3a	Diffuser throat
4	Diffuser trailing edge radius
5	Diffuser exit measurement radius
6	Volute exit
D/S VLS	Vaneless space downsteam of vaned diffuser (4-5)
SVLS	Semi-vaneless space (approx. 3-3a)
U/S VLS	Vaneless space upsteam of vaned diffuser (2a-3)

TECHNICAL ROADMAP

For this research, we primarily consider one, "datum" diffuser geometry: a radial diffuser from a large turbocharger compressor with 17 airfoil shaped vanes (see Figure 2). This is the geometry that is tested back-to-back in the compressor and the swirl rig. Additionally, two further airfoil vaned diffusers are studied numerically. These featured differing inlet stagger, as such defining different diffuser leading edge angles and throat areas (see Figure 2). This can have significant impact on stage performance due to the effect on impeller/diffuser matching, as discussed in [13], and is therefore of interest for this study.

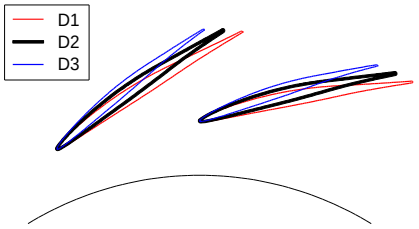

Figure 2: Project diffusers showing how the camber line is altered to vary the throat area. This modifies the leading edge angle. The trailing edge angle is invariant for volute matching. "D" is short for "diffuser" and D2 is the datum geometry.

The datum diffuser is first tested on a compressor test bed, with a stage design stagnation pressure ratio of 5. The diffuser inflow is measured through two specially designed, miniature traversing probes used in the diffuser inlet region. One probe measures total pressure and flow direction across the span at each pitchwise location, while the second records the spanwise variation in total temperature. Four circumferential (pitchwise) positions are measured across one diffuser vane pitch for each operating point (see Figure 4).

A 0.86 scale replica of the diffuser is then tested within the swirling flow test rig. Here, inlet conditions can be replicated from the compressor test facility in terms of average inflow angle and Mach number. The rig features bleed slots at the diffuser inlet that can be used for suction or injection, allowing the time-averaged spanwise flow profiles from the compressor to be approximately replicated within the test rig. However, the unsteady, pitchwise flow non-uniformity imposed by the rotor is different.

The Reynolds number and reduced frequency (defined by the relative timescales of rotor blade passing and the mean throughflow time of the diffuser flow) overlap between the two

[1] A note on figures: The paper introduces plots with relatively unfamiliar ordinates of flow angle and incidence. Our convention is that flow angles are measured from radially outward, with positive being in the direction of impeller rotation. With these ordinates, the positive direction (left to right) is in the direction from choke to stall. Scales are typically removed because the data are from current production turbocharger compressors and are proprietary.

facilities. Table 1 provides a summary of the relevant non-dimensional parameters and flow conditions.

The time-averaged spanwise non-uniformity, together with the time- and spatially averaged inflow angle and Mach number, can be closely matched between the two rigs. This allows the effects of the unsteady pitchwise inflow non-uniformity to be isolated, when comparing the performance of the datum diffuser between the two rigs.

	Compressor	Swirl rig
Scale factor	100%	86%
Re	$2\times10^5 - 5\times10^5$	$1.2\times10^5 - 3\times10^5$
Reduced frequency (bpf)	14 – 15	1.3 – 24
Maximum Mach number	1.2	1.2
Maximum flow angle (from radial)	75°	75°
Flow angle distribution	Up to 35°	Match via control slots
Mach distribution	Continuously varies from 0 – 1.2 across span	Match via control slots
Exit conditions	Volute	Volute

Table 1: Comparison of swirling flow rig and compressor rig

Characterizing the influence of the spanwise inflow non-uniformity is more challenging, since it must be isolated from other effects such as averaged inflow angle or Mach number, or pitchwise non-uniformity. To identify 'similar' inflow conditions with differing distributions of Mach number and flow angle, appropriate spatial averages must be defined. With these averaged values, every operating point in either the compressor or the swirl rig exhibits different time-averaged spanwise profiles.

For further differences in spanwise profile, two other impeller geometries are studied numerically. These are also production turbocharger compressor impellers with approximately the same stage total pressure ratio. However, they are not of evolutionary design but rather are developed independently, and include differing features such as blade count (8 or 9 main blades plus splitters), endwall profiles, trailing edge spans, and twist at the trailing edge, providing a range of different impeller outflows (further discussed below). Table 2 shows the complete matrix of geometries examined in this project.

	Impeller 1	Impeller 2	Impeller 3
Diffuser 1		*CFD only*	
Diffuser 2	*CFD only*	**DATUM** *CFD* *Compressor rig* *Swirl rig*	*CFD only*
Diffuser 3		*CFD only*	

Table 2: Matrix of compressor geometries.

EXPERIMENTAL FACILITIES

The MIT swirling flow diffuser test facility utilized (the "swirl rig") comprises a high-solidity, forward leaning, radial rotor, which can provide a highly swirling, transonic flow for the downstream diffuser. The rotor design aims to minimize the pitchwise variations from the rotor by using 72 negative reaction rotor blades, with the relative velocity continuously rising and the static pressure continuously dropping through the rotor. The design is a modification of that used by Filipenco, described in [3, 14]. Details of the modifications can be found in [15]; these included modification of span-to-radius ratio and the fitting of a turbocharger volute.

Within the swirl rig, the spanwise flow profile into the diffuser can be modified using circumferential slots on the shroud and hub endwalls located upstream and downstream of the swirl generator (see Figure 3). The flow through each of the four slots can be independently controlled with a connection both to a high pressure air supply (for injection) and a low-pressure vacuum system (to withdraw air). The rotor speed is continuously variable from 500 to 7000 RPM, and the rig backpressure can be set either above ambient or below, using a throttle valve and a slave compressor. Using a combination of these settings allow the swirl rig to produce a diffuser inflow representative of the compressor except in pitchwise non-uniformity[2].

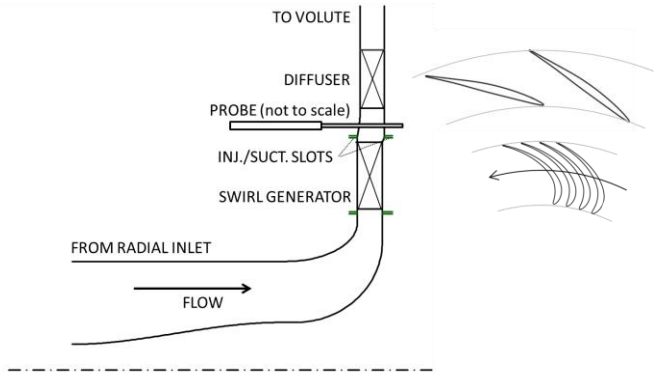

Figure 3: Sketch of swirl rig cross-section and blading

The rig is extensively instrumented with static pressure taps, fast response pressure transducers (for assessment of stall inception, not further discussed in this paper), and thermocouples at the rig inlet and outlet. Static pressure taps recorded diffuser inlet and exit pressure, and two diffuser passages are instrumented per Figure 4 to further break down the pressure rise through the diffuser, typically identified in terms of its subcomponents: upstream vaneless space, semi-vaneless space, diffuser passage, and downstream vaneless space (between the vaned diffuser exit and the volute inlet). Static pressure is recorded using six 16-channel Scanivalve DSA3217 units with a 15 psi range (differential) and an

[2] Local (shroud-side) flow reversal at the diffuser inlet measurement plane observed at some off-design operating points in the compressor proved impossible to replicate in the swirl rig.

accuracy of 0.05% full scale. A calibrated venturi in the exit duct is used for mass flow measurement.

In addition, miniature traversing probes were developed for measurement of the time-average spanwise total pressure, flow angle, and total temperature. In the swirl rig, only the total pressure/angle (p_t/α) probe is used, and the total temperature, measured at the volute exit, is assumed uniform across the span[3]. The probe comprises a 0.8 mm closed tube which spans the diffuser for the entire traverse. A single 0.1 mm hole is drilled perpendicular to the tube axis on one side, and a pressure transducer is close-mounted inside the probe, just outside the diffuser plate, to record the pressure.

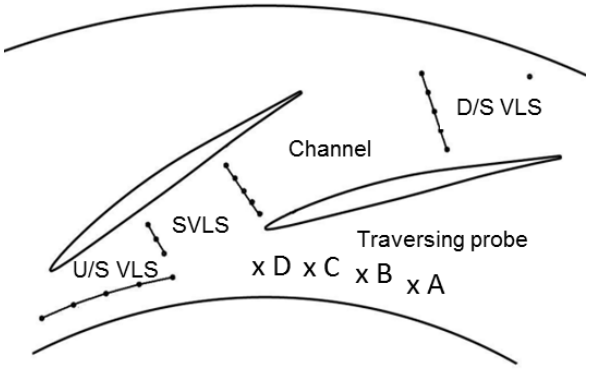

Figure 4: Static pressure taps within a diffuser passage used to break down pressure recovery into subcomponents, together with traverse probe locations A-D (shown in adjacent passage only for illustration).

The p_t/α probe can be mounted in four different circumferential positions equally spaced across one pitch, thus each operating point is repeated four times for the complete diffuser inflow mapping. Since the probe frequency response is typically less than the rotor blade passing frequency, the pitchwise non-uniformity measured is only that caused by the upstream pressure field of the diffuser vanes. At each circumferential position, the probe is moved axially through the diffuser in a number of steps, clustered near the endwalls. At each axial position, the probe is rotated about its principal axis in steps of 15°. The measurements thus taken are subsequently post-processed, in combination with the endwall static pressure measurements, to map the total pressure and the flow angle profiles into the diffuser. The probe accuracy for angle measurement is estimated through controlled wind tunnel tested as ±0.5°.

A second probe was developed to measure spanwise variations in total temperature, but this is only used in the compressor rig, where total temperature varies significantly across the span. This total temperature (T_t) probe comprises a 0.81 mm tube with two aligned holes drilled radially through the tube. The first hole, 0.46 mm in diameter, is rotated to face the direction of the flow (the probe is used following a traverse of the total pressure and flow angle probe). Flow approaching the probe is brought to rest at the thermocouple head and vents through the downwind hole, which is 0.15 mm in diameter. Within the tube a miniature K-type thermocouple is mounted with the exposed bead held between the two holes. The T_t probe is calibrated for temperature recovery factor per [16]. Further information on both traversing probes and their calibration can be found in [15].

The Super-Martin (SUMA) closed loop compressor test facility at ABB Turbo Systems Ltd. in Baden, Switzerland is used for the compressor tests. The compressor has a high swallowing capacity, open impeller, with a design impeller blade Mach number, $M_2 = \Omega r_2/\sqrt{(\gamma R T_{t1})}$, of 1.54 and with 9 backswept and splittered blades. It is electrically driven. The gas circuit contains a water-cooled heat exchanger such that the inlet conditions can be maintained with constant total temperature to within approximately ±1K. The inlet total pressure can also be reduced to sub-ambient to allow operation of the rig at high pressure ratios without excessive power requirements by reducing the inlet air density.

The diffuser is instrumented, as far as possible, identically to the diffuser tested in the swirl rig; however static pressure measurements are taken using ABB's standard data acquisition system, compliant with ISO9001. In addition to the diffuser instrumentation described above, the compressor rig includes multi-point static pressure and temperature measurement in the ducts upstream and downstream of the compressor, and a v-cone to measure mass flow. These data are post-processed with a proprietary meanline data reduction scheme to calculate conditions through the compressor. The maximum measurement errors, to within 95% confidence levels, are ≤ ±1.0% for volume flow, ≤ ±0.2% for total pressure ratio and ≤ ±0.5% for efficiency over the operating range considered within this paper.

The radial spacing between the rotor trailing edge and the diffuser leading edge is 15% of the rotor tip diameter in both the swirl rig and the compressor rig. The diffuser inlet conditions are recorded at a measurement plane which is midway between the rotor and the diffuser. Both endwall static pressure measurement and the traversing probes record data at this radial location.

COMPUTATIONAL APPROACH

Computations are all undertaken using the commercial Reynolds-Averaged Navier Stokes (RANS) CFD code Numeca FINE/Turbo, using a structured hexahedral grid generated with the Numeca tool Autogrid. Unless otherwise noted, the simulations are single-passage, 'phase-lagged' unsteady simulations [17,18] with a computational domain which includes both a single compressor impeller passage (main and splitter blade) and a single diffuser passage.

Grid and timestep convergence studies were undertaken to achieve acceptable accuracy while maintaining manageable convergence times.. This results in a mesh containing 1.4 million cells for the impeller and 0.4 million cells in the

[3] The work done by the swirl rig rotor is low, resulting in total temperature ratios below 1.15. The assumption of uniform total temperature is fair.

diffuser, and a timestep equivalent to 1/36th of the time taken for a main blade to pass by one diffuser pitch.

The Spalart-Allmaras turbulence model is used following successful application in past work [19]. According to best practice, y+ ranges from 1-10 for the first cell off the wall. Unless otherwise specified, the inlet conditions for the stage calculations are defined as uniform and at ambient total conditions i.e. 25°C and 1.03 bar, with an axial velocity vector (i.e. normal to the stage inlet surface). The exit boundary condition enforces a uniform static pressure at diffuser exit. Further details on the numerical approach can be found in [15].

The agreement between computation and measurement, and hence the accuracy of the former, is assessed through evaluation of the stage total pressure ratio and efficiency, impeller outflow average total pressure and flow angle, impeller outflow spanwise profiles (see Figures 5 and **6**), the diffuser static pressure rise coefficient (together with its subcomponents, see Figures 7 and 8), and the diffuser total pressure loss coefficient. Only a sample of this data is shown here; further validation is shown in [15].

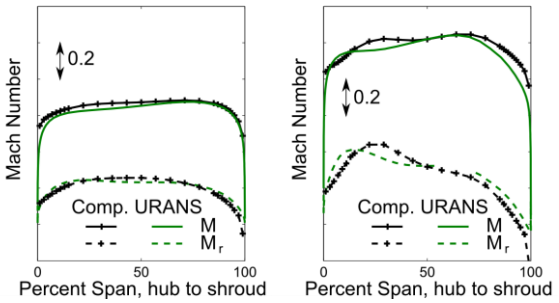

(a) 58% speed, η_{max} **(b) 100% speed, η_{max}**

Figure 5: Spanwise profiles of Mach number and radial component at the diffuser inlet, at mid-pitch, as measured in the compressor versus URANS.

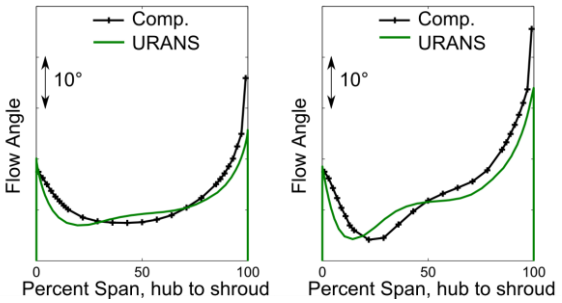

(a) 58% speed, η_{max} **(b) 100% speed, η_{max}**

Figure 6: Spanwise profiles of flow angle at the diffuser inlet, at mid-pitch, as measured in the compressor versus URANS.

Figures **5** and **6** show the good agreement in spanwise profiles observed: the maximum angle difference between experiment and URANS is 5° and the maximum Mach discrepancy is 11%. Similar agreement is obtained across the different pitchwise positions and operating points; the worst agreement is at 100% design speed case in choke, where an angle error of 7° and a Mach error of 30% (in one localized area) occurs.

The static pressure rise through the diffuser is reasonably well estimated within the CFD; neglecting operating points in or near choke, the agreement is within ±7%. Better results are obtained at low compressor speed and toward stall, both of which are indicative of lower diffuser Mach numbers. The results also indicate the challenge in obtaining converging solutions near to stall for the high speed cases.

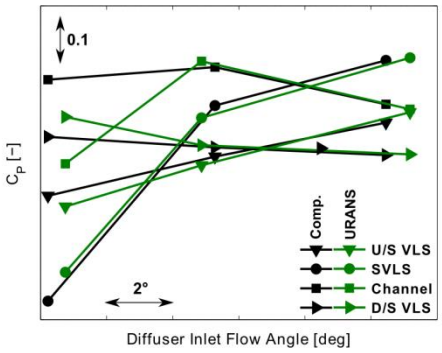

Figure 7: Comparison of diffuser sub-component characteristics recorded in the compressor tests ("Comp.") and calculated in URANS at 58% design corrected speed

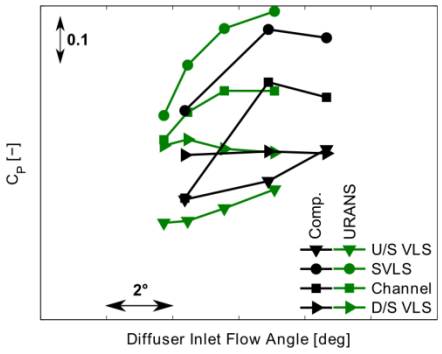

Figure 8: Comparison of diffuser sub-component characteristics recorded in the compressor tests ("Comp.") and calculated in URANS at 100% design corrected speed

At low inflow angles near the choke condition (left side in Figures 7 and 8), the diffuser vane suffers negative incidence stall. This is particularly noticeable in the simulations at 58% design corrected speed, where the URANS simulations show separated flow from the leading edge of the diffuser through the entire diffuser passage. Separation, and the subsequent separated flow, is typically not well captured in RANS modeling [20]. Since large separations are present for all speedlines at the lowest flow angle simulated, the inaccuracy in the modeling of the separated flow is likely the cause for the differences between experiment and the URANS results. Additionally, shock waves that develop within the diffuser may not be well captured with the relatively coarse mesh utilized for the unsteady CFD. Supporting this hypothesis, it can be

observed that the diffuser channel, with the largest extent of flow separation, is the subcomponent which shows the largest discrepancy.

AVERAGING AND PERFORMANCE METRICS

The typical metric for diffuser performance is the pressure recovery coefficient, C_p, which is defined as the static pressure rise $p_5 - p_{2a}$ as a fraction of the inlet dynamic pressure, $p_{t2a} - p_{2a}$ [2,12]. The limitations of this definition, when used for a radial vaned diffuser, are that (a) the diffuser pressure recovery can depend on Mach number, due to density changes through the diffuser; (b) it takes no account of the change in the effective diffuser area ratio as the flow into the diffuser becomes more tangential, which has the effect of reducing the streamtube area into the diffuser and thus the contraction or expansion of the flow from the impeller trailing edge to the diffuser throat.

An alternative metric is the diffuser effectiveness [21], which is the ratio of the diffuser static pressure rise to that of an ideal, quasi-one-dimensional, diffuser. This is developed for the application of radial compressors with compressible, non-uniform, swirling inflow as follows:

It is assumed that the ideal area ratio of the diffuser is defined by Equation 2:

$$AR = \frac{A_{5,eff}}{A_{2,eff}} = \frac{r_5}{r_{2a}} \frac{b_5}{b_{2a}} \frac{\cos \chi_4}{\cos \alpha_{2a}} \qquad (2)$$

This is the "ideal" streamtube through the diffuser, defined using the measured average diffuser inflow angle and the diffuser vane trailing edge angle (i.e. the Kutta condition applied to the diffuser vane and assuming flow angles do not change significantly between the trailing edge and the diffuser exit, which is a good assumption for the low Mach number typically encountered downstream of the vaned portion).

For the ideal case, the inlet Mach number and flow angle are taken as their average values and the flow is quasi-steady, such that any $\partial/\partial t$ terms can be neglected.

The area ratio (Equation 2) allows the ideal exit Mach number, $M_{5,i}$, to be calculated using the compressible flow function $D(M)$ as in Equation 3:

$$D(M_{5,i}) = \frac{\gamma}{\sqrt{\gamma - 1}} M_{5,i} \left(1 + \frac{\gamma - 1}{2} M_{5,i}^2\right)^{-\frac{\gamma+1}{2(\gamma-1)}} = \frac{D(M_{2a})}{AR} \qquad (3)$$

Using the ideal exit Mach number, and setting total pressure losses to be zero, it is possible to determine an ideal pressure rise for the diffuser for any inlet Mach number and flow angle using the isentropic relationship $\frac{p}{p_t} = f(M)$.

The second diffuser performance metric used is the total pressure loss coefficient $C_{p,t}$. This is defined as the total pressure reduction $p_{t,2a} - p_{t,5}$ as a fraction of the inlet dynamic pressure. This represents the losses (or entropy gain) through the diffuser.

The remaining performance metric for the diffuser, for fully characterization, is the remaining kinetic energy in the flow at its outlet. However it is possible to derive this from the other two metrics, for a diffuser operating with ideal gas.

The average inflow Mach number and flow angles used within the performance metrics are taken to be the mixed out average [2,5,22]. This is further discussed in the following section. For calculating the total pressure loss coefficient and the dynamic pressure at diffuser inlet, the average total pressure is taken as the mass average; the "correct" choice is the entropy or availability average, but the mass average is more readily measured and is typically similar [3,5].

EFFECT OF TIME-AVERAGE MACH NUMBER AND FLOW ANGLE

Rather than examine pitchwise non-uniformity first, it is informative to assume that it has no impact on diffuser performance then challenge that assumption later. This provides insight that clarifies the later discussion.

Ten operating points are studied in the compressor tests: near choke (CH), near stall (ST) and near best efficiency (η_{max}), for three different design corrected speeds. Diffuser pressure recovery and effectiveness are calculated, as are average inflow parameters such as the momentum average flow angle, the mixed out average flow angle, and the average Mach number. The correlation proposed by Filipenco [3] is tested with this diffuser, but is found to suffer from a large spread as previously shown in Figure 1; 17.7% variation in pressure recovery is experienced within a momentum averaged angle difference within one degree, around the η_{max} operating point.

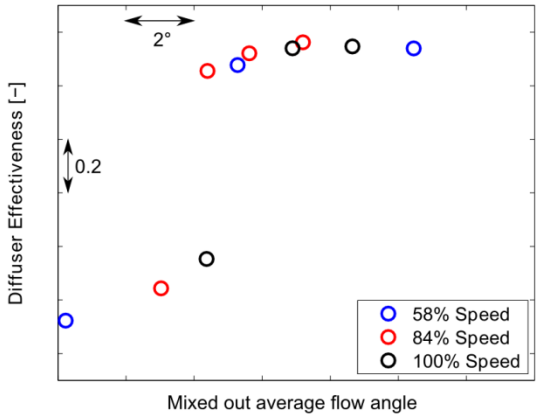

Figure 9: Results from the compressor test, showing diffuser effectiveness correlates well with mixed out average flow angle.

Figure 9 shows that the data collapses if effectiveness is used as the performance metric, and the mixed out average angle as the correlating function. The exceptions are the CH operating points. The use of different speeds in the compressor means that a range of different inflows in terms of Mach number, non-uniformity and unsteadiness are encountered. It is found that the use of the mixed out average resolves issues of different non-uniformities and unsteadiness, and that using

effectiveness improves the correlation of results at significantly different Mach numbers. At low flow angles (CH operating points), the data is scattered, and this is discussed later.

To further test the correlation, the results from the CFD simulations are added to the plot in Figure 10. Here, all three impeller geometries (I1, I2 and I3) are matched with the same diffuser. Figure 11 shows a sample of the computed spanwise profiles which are used. The CFD data further support the correlation, with the same exception as observed earlier for the cases with low average diffuser inflow angles.

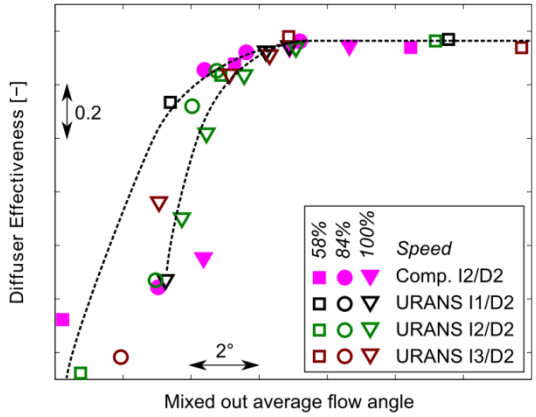

Figure 10: Results from URANS simulations added to the results from the compressor tests ("Comp"), at three different compressor design corrected speeds

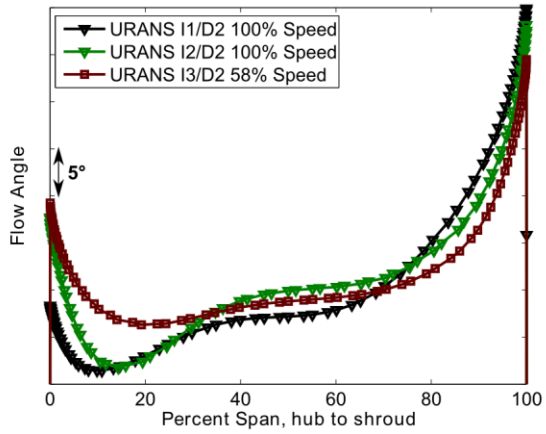

Figure 11: Spanwise profiles of flow angle at mid-pitch for three URANS cases at the same mixed out average angle, showing a variety of blockage and skew which obtain comparable pressure recoveries

As observed by Filipenco and Deniz [3,4], the emphasis placed on blockage in typical approaches to the analysis of vaned diffusers appears misplaced. Mixing occurs through the vaneless space between impeller and diffuser; CFD data shows that, for the peak efficiency point at the design corrected speed, the non-uniformity in mass flux reduces by 7% from impeller trailing edge to the diffuser trailing edge. This contrasts with a steady, non-mixing flow through a diffuser, where flow non-uniformity worsens, causing poor pressure recovery and potential flow reversal (see, for example, [22]).

The total pressure losses shown in Figures 12 and 13 take the form of familiar loss buckets from cascade airfoil tests, with the region of minimum loss narrowing with increased Mach number. Minimum loss occurs at a small positive incidence, and loss increases rapidly with reducing incidence (i.e. negative incidences). This is due to a large region of separated flow on the pressure side of the diffuser vane. On the side of positive incidence, rather than showing increased loss (the right-hand side of the bucket), instead the compressor stalls (or CFD simulations fail to converge, which is taken as a crude proxy for compressor instability). Between, there is a flat region of minimum loss.

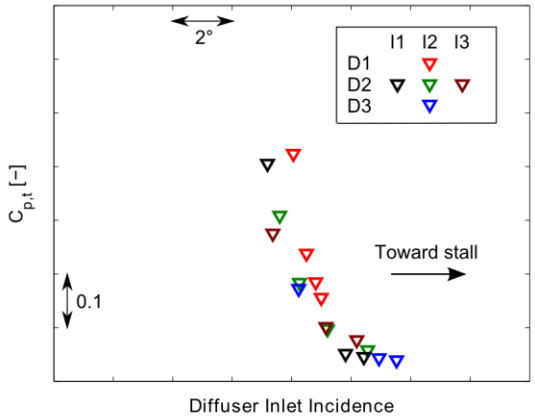

Figure 12: Total pressure loss coefficient ($C_{p,t}$) as a function of diffuser inlet incidence, showing a classic 'loss bucket' shape similar to cascade airfoil data; diffuser inflow Mach numbers >0.8, and impeller/diffuser combinations as indicated by the legend.

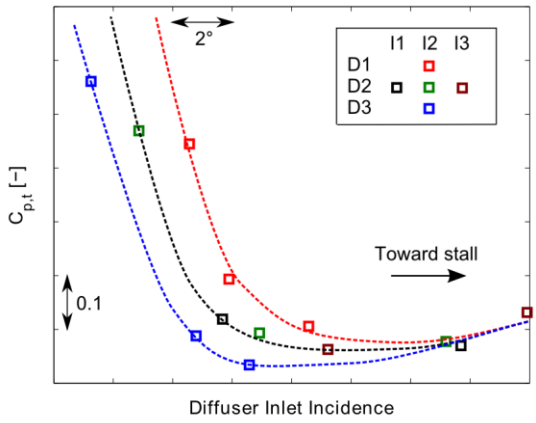

Figure 13: $C_{p,t}$ as a function of diffuser inlet incidence for diffuser inflow Mach numbers from 0.5 to 0.8, showing greater sensitivity to secondary effects such as diffuser loading distribution.

The rapid increase in loss, caused by separation at negative incidence, is the cause for the rapid degradation of effectiveness at low angles shown in Figure 10. The correlation at high Mach number across all the diffuser geometries supports the

hypothesis that the loss is driven by incidence (rather than, for example, purely the flow angle), since the different diffusers have different leading edge angles. At lower speeds, other sources of loss become relatively more important; examples include the greater flow path or longer chord (and hence wetted diffuser surface) for diffuser 1 relative to diffuser 3, which are byproducts of the different camber, or the differences in loading distribution, since diffuser 1 tends to be more aft-loaded. Subsequent work has further explored this topic [23].

For both Figures 12 and 13, only CFD data are shown. The exit total pressure is not recorded in experiments until downstream of the volute. As such it is not possible to isolate diffuser loss from volute losses. Trends between experiment and CFD data are similar, as can be observed later in Figure 19, except for an offset which is proportional to the kinetic energy of the diffuser exit flow. Matching with the volute is discussed in [12] and [23].

To return to the original hypotheses, the data does not support that the spanwise flow profile has much impact on the performance of the diffuser, except as it affects the mixed out average conditions. This supports the general findings of Filipenco and Deniz [3,4], although the mixed out average angle is determined to be more generally applicable than the momentum averaged angle used by these two authors. Taken in combination with their data, three very different diffuser geometries are tested (a pipe diffuser, a wedge-vaned channel diffuser, and a relatively low solidity, airfoil vaned diffuser), suggesting generality to the result. However, each has a vaneless space 10% of the impeller tip radius or greater, which may allow for greater mixing than a more close-coupled compressor.

Additionally, the data reveals a consistent, measureable impact of Mach number on the pressure recovery, counter to the conclusion of some other researchers, for example [4]. The impact is small, approximately a difference of 10% in pressure recovery for Mach numbers varying from 0.5 to 1.0. It can be quantified using a quasi-one-dimensional analysis of the diffuser, using the assumption of a mixed out state at diffuser inlet.

EFFECTS OF PITCHWISE NON-UNIFORMITY

Data from the swirl rig indicate that the diffuser effectiveness and total pressure loss remains well correlated to the mixed out average angle. The diffuser performance is very similar between the compressor tests and the swirl rig tests, except as the compressor approaches high flow angles[4]. Here, diffuser effectiveness is greater in the swirl rig, as shown in Figure 14, which can be related to a higher total pressure loss in the compressor, as shown in Figure 15.

To isolate the cause of this discrepancy, an operating point representative of the 58% design corrected speed, near stall point in the compressor is reproduced as closely as possible within the swirl rig. This is achieved through careful adjustment of the rotor speed and volute backpressure, together with application of cross-flow suction and injection through the endwall slots upstream of the diffuser section. The mixed out average inflow angle and Mach number agree to within less than 0.1° and 4% respectively (the Mach number being lower in the swirl rig). Comparing the spanwise flow profiles between the compressor and the swirl rig for this operating point in Figure 16, the agreement is qualitatively good.

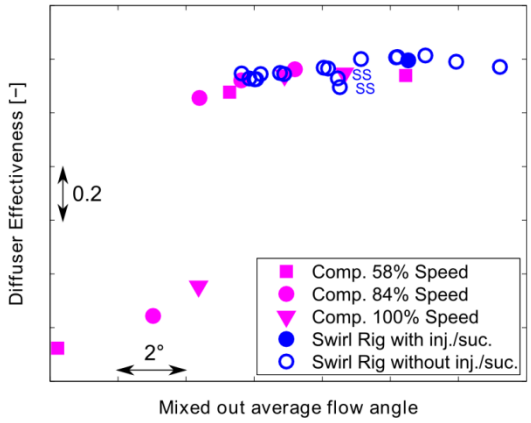

Figure 14: Diffuser effectiveness in the compressor tests ("Comp.") and the swirl rig, showing generally good correlation. An exception is where the swirl rig rotor is choked, leading to supersonic diffuser inlet flow ("SS").

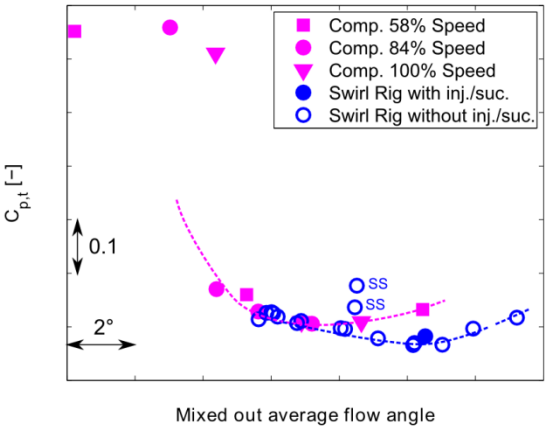

Figure 15: Diffuser and volute $C_{p,t}$ in the compressor tests ("Comp.") and the swirl rig. A clear difference exists between the two machines at high angles.

The diffuser effectiveness and total pressure loss coefficient measured in the swirl rig with this matched condition are 0.06 higher and 0.05 lower respectively than that measured in the compressor. This is shown in Figures 14 and 15 using a solid symbol; all other data points have no injection or suction present. The estimated experimental errors in flow angle, effectiveness, and total pressure loss coefficient (once the uncertainty from the instrumentation is propagated through the post-processing calculations) are ±0.6°, ±0.013, and ±0.003

[4] The high forward lean in the swirl generator meant that it is not possible to achieve low flow angles.

respectively. The differences are clearly larger than can be explained due to these errors.

The reduced frequency in the two tests (defined as the diffuser through-flow time relative to a blade passing period) is 8% different. The Reynolds number is 42% lower in the swirl rig; while this is a significant difference, the higher Reynolds number in the compressor suggests lower loss (by approximately 9%, according to the method of Strub et al. [24]) rather than the opposite as observed.

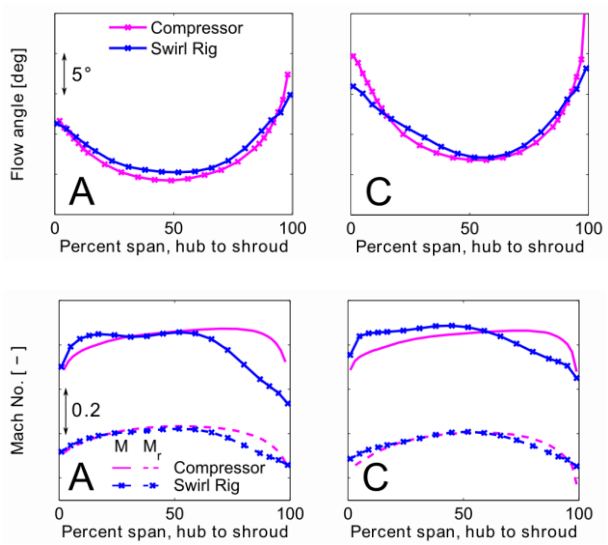

Figure 16: Spanwise profiles of flow angle (top) and Mach number including radial component (bottom), for a matched operating point representative of the compressor 58% speed, η_{max} operating point. "A" and "C" represent pitchwise positions per Figure 4.

We posit that the only major difference between the two tests is in the magnitude of the unsteady pitchwise non-uniformity from the rotor. It is proposed that the compressor has a higher loss than the swirl rig at high angles due to the unsteady fluctuation of incidence and the non-linearity of the loss curve at high angles. At 58% design corrected speed, near stall, RANS simulations[5] show the compressor impeller outflow has fluctuations in flow angle of 35° across a rotor blade pitch, whereas the swirl rig is relatively uniform with variations of less than 5°, as indicated in Figure 17.

While the diffuser is operating at a time-averaged incidence near the center of the relatively flat region of minimum loss, the diffuser in the swirl rig and the compressor achieve similar performance. At the edges of the loss bucket, loss begins to increase rapidly with changes in incidence (this is observed at low time-average incidences but not at high incidence as the increased loss triggers compressor instability). This means that angle variations at the diffuser inlet will have a non-linear response in terms of loss, such that a flow matched on the basis of the time-averaged inflow angle will not have the same loss coefficient. This is sketched in Figure 18.

[5] RANS simulations of the isolated impeller are shown in [15] to provide a similar impeller outflow as in the stage URANS simulations, at low speeds.

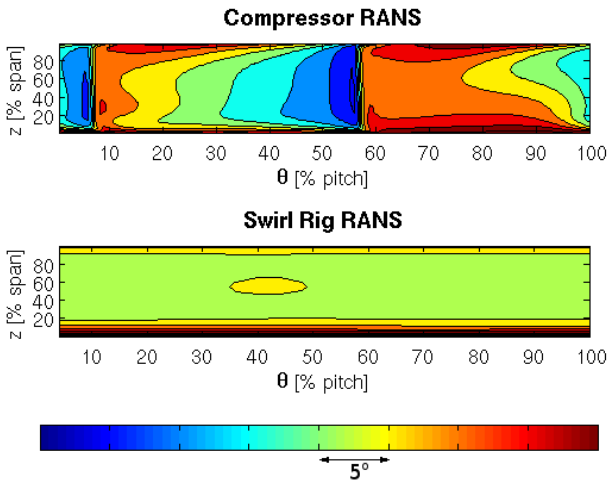

Figure 17: Angle variations at rotor exit (1.02% r_2) for the compressor impeller and the swirl generator, for vaneless diffuser RANS simulations i.e. isolated rotors, at average conditions representative of the compressor 58% speed η_{max} operating point.

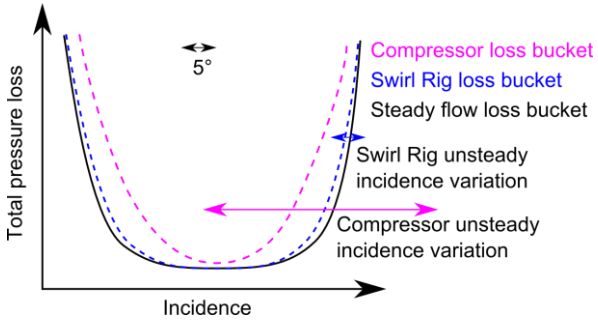

Figure 18: Sketch indicating the hypothesized mechanism by which unsteady angle variations increase total pressure loss relative to a steady flow.

A mixing analysis supports this hypothesis and reveals that the increased magnitude of the pitchwise non-uniformity from the rotor encountered toward stall does not lead to sufficiently increased loss to explain the discrepancy, noting that except at high angles, the two machines are in close agreement. Additionally, using the instrumented diffuser passage, the reduced pressure recovery in the compressor test can be localized to regions downstream of the diffuser leading edge (not shown here), again consistent with an incidence effect.

Additional CFD simulations are performed of the diffuser only (from the impeller trailing edge location) in order to quantify the differences in performance for a steady flow relative to that recorded in the previously discussed unsteady simulations. In the steady, diffuser-only simulations, a time-average 2D flow field (varying in pitch and span, but not in time) is applied as an inlet condition, with the recorded impeller outflow from the unsteady simulations mixed out over time at every (z, θ) location. This includes total pressure, total temperature, as well as a flow angle definition and the turbulence viscosity. To support the hypothesis that the

difference observed between the compressor test and the swirl rig test is due to an unsteady incidence variation, the data should show reduced loss in the steady simulation relative to the unsteady one at high inflow angles. However, what is observed in Figure 19 is that the diffuser-only simulations yield a similar level of loss compared to the URANS simulations throughout the operating range. The increased loss may not be captured in the URANS simulation simply due to the limitations of RANS modeling, given that what is expected is an unsteady separation phenomenon. It is also possible that the effect of unsteadiness occurs at a different frequency than is allowed within a single passage, phase-lagged simulations; periodic unsteady phenomena uncorrelated to the frequency of the rotor blade passing was recently observed in work by Anish et al. [25].

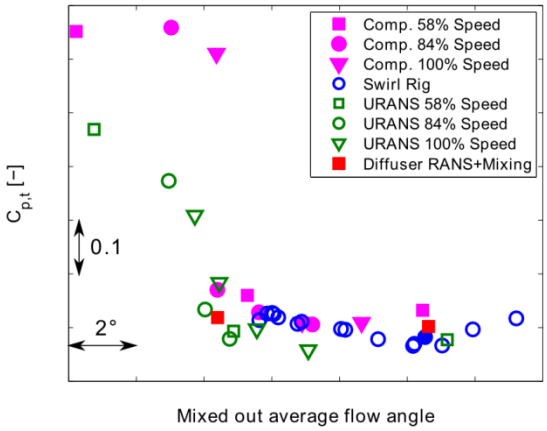

Figure 19: Diffuser and volute $C_{p,t}$ for the compressor and swirl rigs, and diffuser $C_{p,t}$ for stage URANS and diffuser-only RANS CFD. Stage CFD results, once adjusted for the losses inherent in the application of a mixed out inlet condition, agree with the diffuser-only CFD across the operating range.

In summary, the hypothesis that the unsteadiness from the impeller has negligible influence on the diffuser aerodynamics is partially validated: across much of the operating range, around the best efficiency point, this is true. At higher incidence angles towards stall, this is not the case, whereas toward the choke side, insufficient data exist from this project.

CONCLUSIONS

This paper quantifies the relative importance of a number of flow features in radial vaned diffusers. The following conclusions are made:

1. Effectiveness provides an appropriate performance metric across the full range of sub- and transonic Mach numbers. The non-uniform diffuser inflow is accounted for via the use of mixed-out average flow conditions.
2. Effectiveness is well correlated to the mixed out average flow angle. Diffuser performance is shown therefore to be independent of the time-averaged spanwise non-uniformity at the diffuser inlet. This is consistent with the work of Filipenco, Deniz et al. [3,4] but also furthers that work: apart from extending the study to an additional diffuser geometry, the parameters are refined and greater fidelity exists in the measurements.
3. The results enable a ranking to be undertaken for the relative importance of different features of inflow: (1) flow angle, or more specifically the incidence presented to the diffuser vane; (2) Mach number; (3) pitchwise non-uniformity; (4) spanwise non-uniformity.
4. In terms of the features present in the diffuser inflow (i.e. not geometric parameters within the diffuser), incidence is proposed as the primary driver of diffuser performance. This drives separation through the diffuser at off-design conditions, increasing loss and reducing pressure recovery.
5. Mach number effects are most pronounced at low incidence, consistent with a narrowing of the diffuser loss bucket. A similar effect is expected at high incidence, but in the experiments here, the increased loss leads to system instability i.e. stall/surge.
6. Mach number effects are present, but are not pronounced, near design incidence, with additional diffusion at higher Mach numbers consistent with gas density changes. This is captured via a quasi-one-dimensional ideal diffuser analysis, providing the denominator within the chosen definition of effectiveness.
7. Across approximately two-thirds of the operating range, expressed in terms of diffuser inflow angle, the diffuser performance is independent of time-resolved pitchwise non-uniformity (i.e. unsteadiness arising from the upstream rotating blade row). At high incidence angles, it is proposed that the non-linearity of the loss curve together with variations in flow angle from the impeller lead to greater loss.

IMPLICATIONS FOR COMPRESSOR DESIGN

The conclusions above allow recommendations to be made concerning the design of radial compressors. The recommendations are focused on improvements to the diffuser performance, consistent with the research focus here, but the implications of these recommendations on the matched components (particularly the impeller, but also a volute) are also considered. One caveat here is that the recommendations apply to a diffuser with a vaneless space between impeller trailing edge and diffuser leading edge of $0.1r_2 - 0.15r_2$, consistent with the designs of Filipenco [14], Deniz [4], and those considered in this paper.

- The insensitivity to pitchwise non-uniformity across much of the operating range suggests designing the impeller to achieve pitchwise uniformity within the outflow is not necessary for the purposes of diffuser performance, except as it affects the average angle and Mach number.
- In operating conditions where the flow from the impeller provides an unmatched flow angle to the diffuser (i.e. high positive or low negative incidence), strategies to reduce the unsteady flow angle variations are recommended over, for example, reducing wake deficit area.

- In terms of diffuser design, matching the vane incidence with impeller outflow is critically important[6]. This is not a new finding (see, for example, [12]) but is highlighted again by this research.
- Diffuser design approaches that seek low steady-flow losses over a wide range of incidence are recommended, rather than, for example, seeking lowest possible loss across small range. This is in order to accommodate the unsteady variations in incidence without system instability or excessive losses when operating with the transient outflow from the upstream rotor.
- For low Mach number diffusers in particular, performance can be improved through preferentially loading the front of the diffuser, in common with other compressor design practice. This can be achieved through area scheduling as reported in subsequent work [23].
- A hybrid diffuser design approach, leveraging effectiveness, a 'diffuser-as-channel' parameter, together with incidence, a 'diffuser-as-airfoil' parameter, is recommended for further research and development. One potential development route would be to develop a semi-empirical database (similar to those used for channel diffusers or airfoils), using effectiveness and incidence. Isolated diffuser CFD or swirl rig experiments could be used, since inflow non-uniformity has only small effect.

ACKNOWLEDGMENTS

Prof. N. Cumpsty, Prof. E. Greitzer and Dr. R. Hunziker helped shape this research and are thanked for their comments and suggestions throughout the project. James Letendre and Andras Kiss are gratefully acknowledged for their practical assistance during the project, while Dominique Hoskin helped run some of the CFD. The research was funded by ABB Turbo Systems Ltd, which is gratefully acknowledged.

REFERENCES

[1] Reneau, L., Johnston, J., and Kline, S., 1967, "Performance and design of straight, two-dimensional diffusers," Journal of Basic Engineering, vol. 89, p 141.

[2] Japikse, D., 1996, "Centrifugal Compressor Design and Performance", Concepts ETI, Inc.

[3] Filipenco, V.G., Deniz, S., Johnston, J.M., Greitzer, E.M., and Cumpsty, N.A., 2000, "Effects of Inlet Flow Field Conditions on the Performance of Centrifugal Compressor Diffusers: Part 1 - Discrete-Passage Diffuser," ASME J. Turbomach.,122, pp. 1-10.

[4] Deniz, S., Greitzer, E.M., and Cumpsty, N.A., 2000, "Effects of Inlet Flow Field Conditions on the Performance of Centrifugal Compressor Diffusers: Part 2 – Straight-Channel Diffuser," ASME J. Turbomach., 122, pp. 11-21.

[5] Cumpsty, N., and Horlock, J., 2006, "Averaging non-uniform flow for a purpose," J. Turbomach., 128(1), pp. 120-129.

[6] Spakovszky, Z.S. and Roduner, C.H., 2009, "Spike and Modal Stall Inception in an Advanced Turbocharger Centrifugal Compressor", ASME J. Turbomach., 131(3), 031012.

[7] Marconcini, M., Rubechini, F., Arnone, A., and Ibaraki, S., 2010, "Numerical analysis of the vaned diffuser of a transonic centrifugal compressor," ASME J. Turbomach., 132(4), p. 041012.

[8] Cukurel, B., Lawless, P.B., and Fleeter, S., 2010, "Particle Image Velocity Investigation of a High Speed Centrifugal Compressor Diffuser: Spanwise and Loading Variations," ASME J. Turbomach, 132(2), p. 021010.

[9] Wilkosz, B., Zimmermann, M., Schwarz, P., Jeschke, P., and Smythe, C., 2014, "Numerical investigation of the unsteady interaction within a close-coupled centrifugal compressor used in an aero engine," J. Turbomach., 136(4), p. 041006.

[10] Trébinjac, I., Rochuon, N., Kulisa, P., and Bulot, N., 2009, "Effect of unsteadiness on the performance of a transonic centrifugal compressor stage," J. Turbomach., 131(4), p. 041011.

[11] Baghdadi, S., 1977, "The Effect of Rotor Blade Wakes on Centrifugal Compressor Diffuser Performance - A Comparative Experiment", J. Fluids Engineering, 99, pp. 45-52.

[12] Cumpsty, N., 2004, "Compressor Aerodynamics", Reprint Edition, Kreiger Publishing Company, Malabar, Florida.

[13] Casey, M., and Rusch, D., 2014, "The Matching of a Vaned Diffuser With a Radial Compressor Impeller and Its Effect on the Stage Performance," J. Turbomach., 136(12) p. 121004.

[14] Filipenco, V., 1991, "Experimental investigation of flow distortion effects on the performance of radial discrete-passage diffusers," GTL Report 206, Gas Turbine Laboratory, Massachusetts Institute of Technology, Cambridge, MA.

[15] Everitt, J.N., 2014, "The Role of Impeller Outflow Conditions on the Performance and Stability of Airfoil Vaned Radial Diffusers", PhD dissertation, MIT Dept. Aero/Astro.

[16] Arts, T., 1994, "Measurement techniques in fluid dynamics: an introduction; course notes prepared by members of VKI faculty", Von Karman Institute for Fluid Dynamics, Rhode-Saint-Genése, Belgium.

[17] Numeca International, 2013, "Fine Turbo v9.0 User Manual", Brussels, Belgium.

[18] Numeca International, 2013, "Fine Turbo v9.0 Theoretical Manual", Brussels, Belgium.

[19] Everitt, J.N. and Spakovszky, Z.S., 2012, "An Investigation of Stall Inception in Centrifugal Compressor Vaned Diffuser", J. Turbomach., 135(1) p. 011025.

[20] Denton, J., 2010, "Some Limitations of Turbomachinery CFD," ASME Paper No. GT2010-22540.

[21] Sovran, G., and Klomp, E., 1967, "Experimentally determined optimum geometries for rectilinear diffusers with rectangular, conical or annular cross-section," Fluid Mechanics of Internal Flow.

[22] Greitzer, E.M., Tan, C.S., Graf, M., 2004, "Internal Flow: Concepts and Applications", Cambridge University Press, Cambridge, UK.

[23] Gao, R., and Spakovszky, Z.S., 2016, "Area-Schedule Based Design of High Pressure Recovery Radial Diffusion Systems", ASME Paper No. GT2016-57044.

[24] Strub, R.A., Bonciani, L., Borer, C.J., Casey, M.V., Cole, S.L., Cook, B.B., Kotzur, J., Simon, H., and Strite, M.A., 1987, "Influence of the Reynolds number on the performance of centrifugal compressors," J. Turbomach., 109(4), pp. 541-544.

[25] Anish, S., Sitaram, N., and Kim, H., 2014,"A numerical study of the unsteady interaction effects on diffuser performance in a centrifugal compressor," J. Turbomach., 136(1), p. 011012.

[6] Matching the diffuser throat area for the required operating range is also of critical importance although it is not explicitly discussed within this paper.

